
# Supporting Information

for *Macromol. Biosci.*, DOI: 10.1002/mabi.202000183

# Rheological Properties of Coordinated Physical Gelation and Chemical Crosslinking in Gelatin Methacryloyl (GelMA) Hydrogels

Ashlyn T. Young, Olivia C. White, and Michael A. Daniele*

# *Rheological properties of coordinated physical gelation and chemical crosslinking in gelatin methacryloyl (GelMA) hydrogels*

*By Ashlyn T. Young[1], Olivia White[2], and Michael A. Daniele[1,2]**

[1] Joint Department of Biomedical Engineering
North Carolina State University and University of North Carolina, Chapel Hill
911 Oval Dr., Raleigh NC, 27695 (USA)
[2] Department of Electrical & Computer Engineering
North Carolina State University
890 Oval Dr., Raleigh NC, 27695 (USA)

[*] Correspondence: mdaniel6@ncsu.edu

**List of Supplementary Materials:**
Figures S1-S13

## SUPPLEMENTARY FIGURES

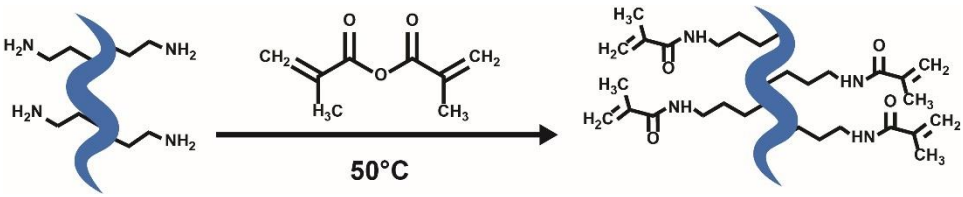


**Figure S1.** Synthesis of gelatin methacryloyl (GelMA).

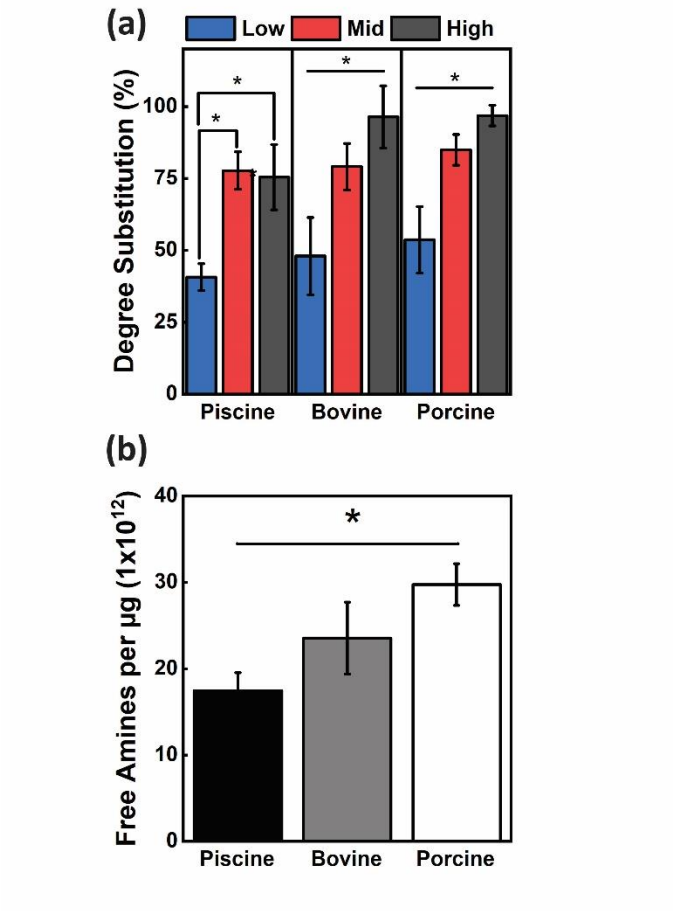


**Figure S1.** (a) DS significantly increases with increasing amount of methacrylic anhydride reacted with unmodified gelatin, except for cold-water fish GelMA that reached a maximum DS around 75%. (b) Free amines available on unmodified gelatin differs depending on animal source and Bloom strength, with porcine gelatin possessing the highest quantity of primary amines, and piscine gelatin possessing the least. Statistical analysis included t-test comparisons with a p-value of 0.05 (n=9). Error bars are plotted as the standard deviation.

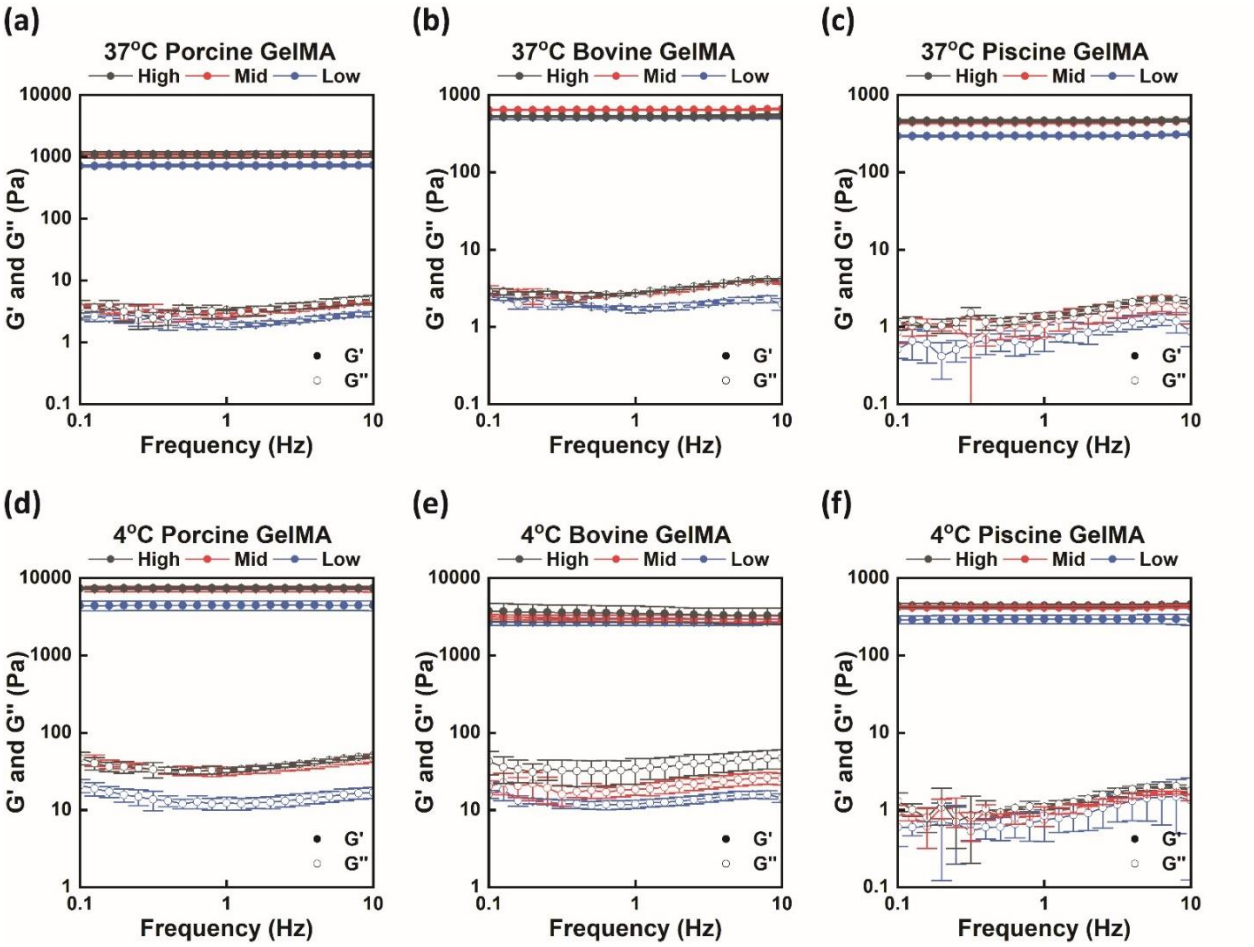


**Figure S3.** Storage modulus (G') and loss modulus (G'') of GelMA samples from 0.1 Hz to 10 Hz for (a) porcine GelMA polymerized at 37°C, (b) bovine GelMA polymerized at 37°C, (c) piscine GelMA polymerized at 37°C, (d) porcine GelMA polymerized at 4°C, (e) bovine GelMA polymerized at 4°C, and (f) piscine GelMA polymerized at 4°C.

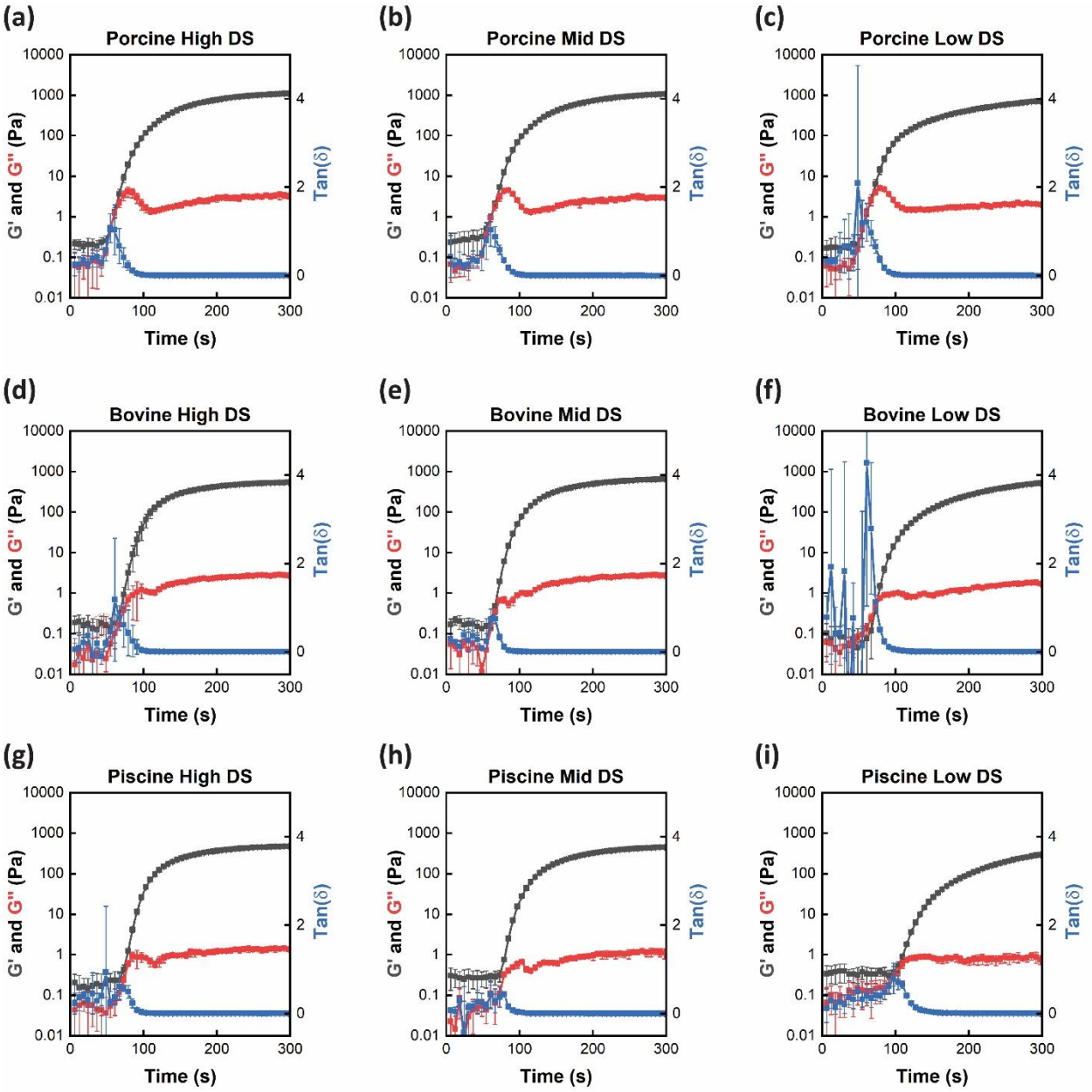


**Figure S4.** Storage modulus (G'), loss modulus (G'') and tan(δ) of GelMA samples over 5 minutes polymerized at 5 mW $cm^{-2}$ after incubation at 37°C for (a) High DS porcine GelMA, (b) Mid DS porcine GelMA , (c) Low DS porcine GelMA, (d) High DS bovine GelMA , (e) Mid DS bovine GelMA (f) Low DS bovine GelMA, (g) High DS piscine GelMA, (h) Mid DS piscine GelMA, and (i) Low DS piscine GelMA.

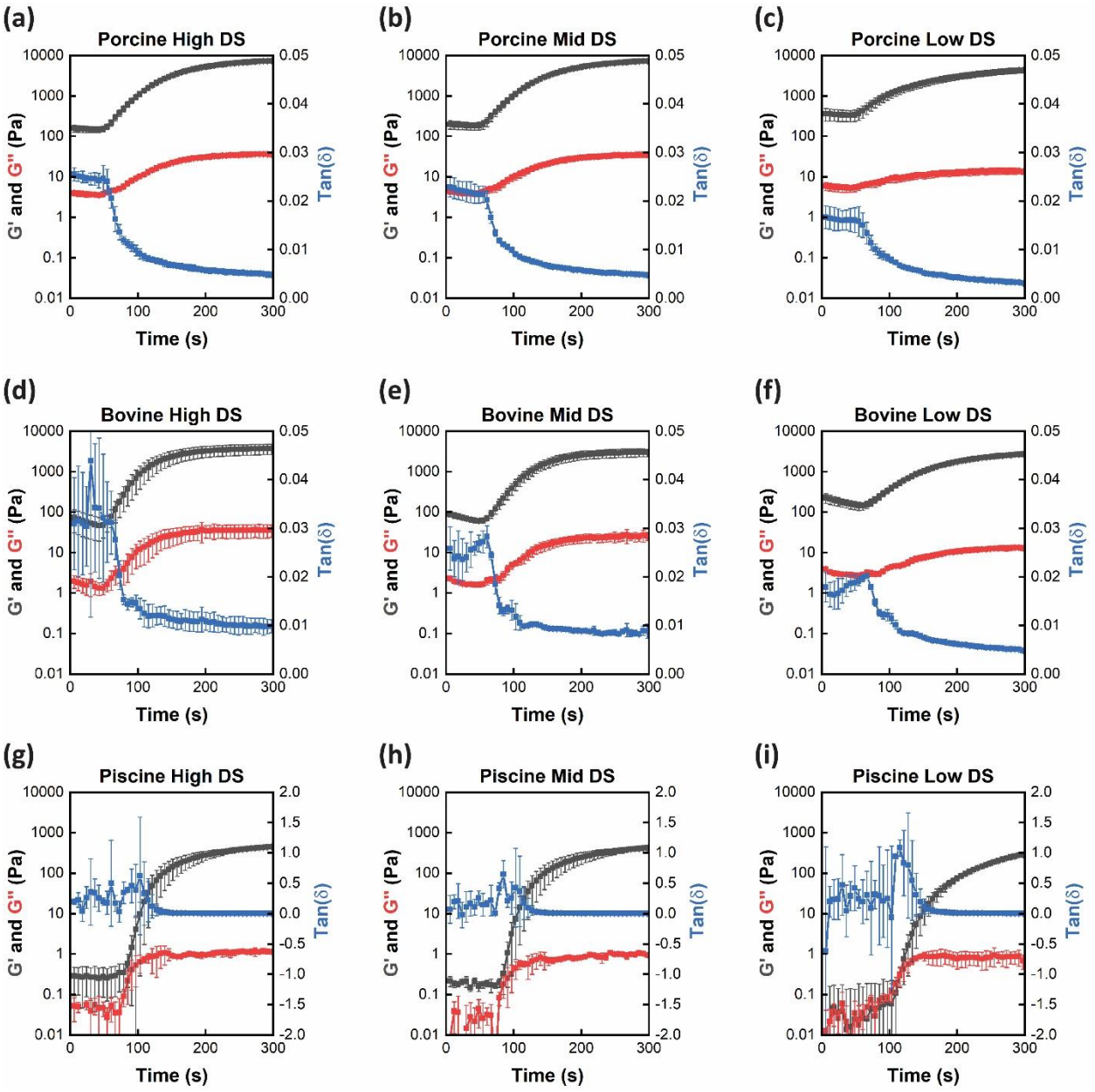


**Figure S5.** Storage modulus (G'), loss modulus (G'') and tan(δ) of GelMA samples over 5 minutes polymerized at 5 mW $cm^{-2}$ after incubation at 4°C for (a) High DS porcine GelMA, (b) Mid DS porcine GelMA , (c) Low DS porcine GelMA , (d) High DS bovine GelMA , (e) Mid DS bovine GelMA (f) Low DS bovine GelMA, (g) High DS piscine GelMA, (h) Mid DS piscine GelMA, and (i) Low DS piscine GelMA.

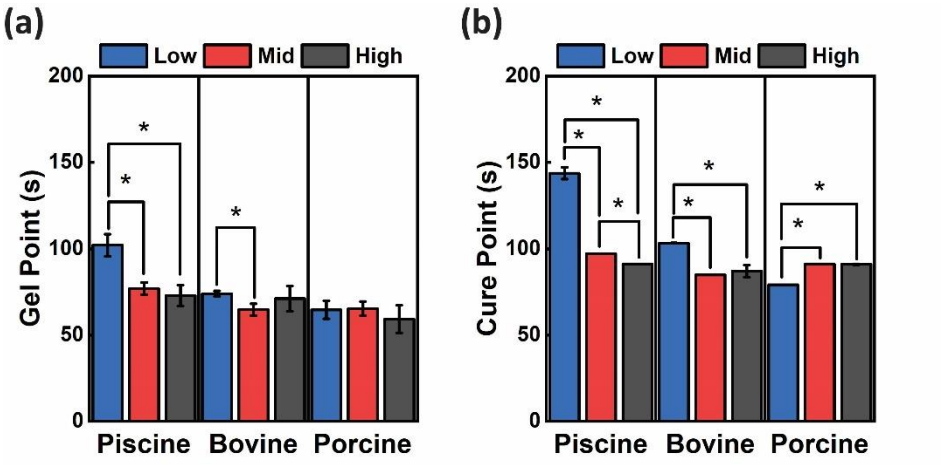


**Figure S6.** (a) Gel points and (b) Cure points calculated from UV polymerization rheology of samples crosslinked at 37°C for piscine, bovine, and porcine GelMA at low, mid, and high degrees of substitution.

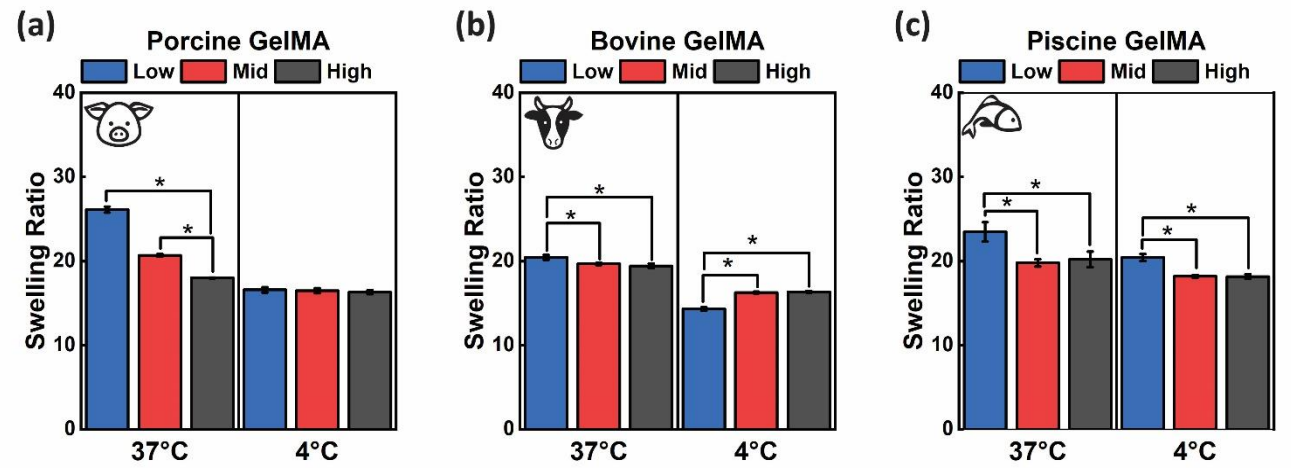


**Figure S7.** Swelling ratios for (a) porcine GelMA (b) bovine GelMA and (c) cold water fish GelMA were directly correlated to storage modulus (G'), as demonstrated by reduced swelling for samples polymerized at 4°C and increase swelling for samples polymerized at 37 °C. Statistical analysis included t-test comparisons with a p-value of 0.05 (n=9). Error bars are plotted as the standard deviation.

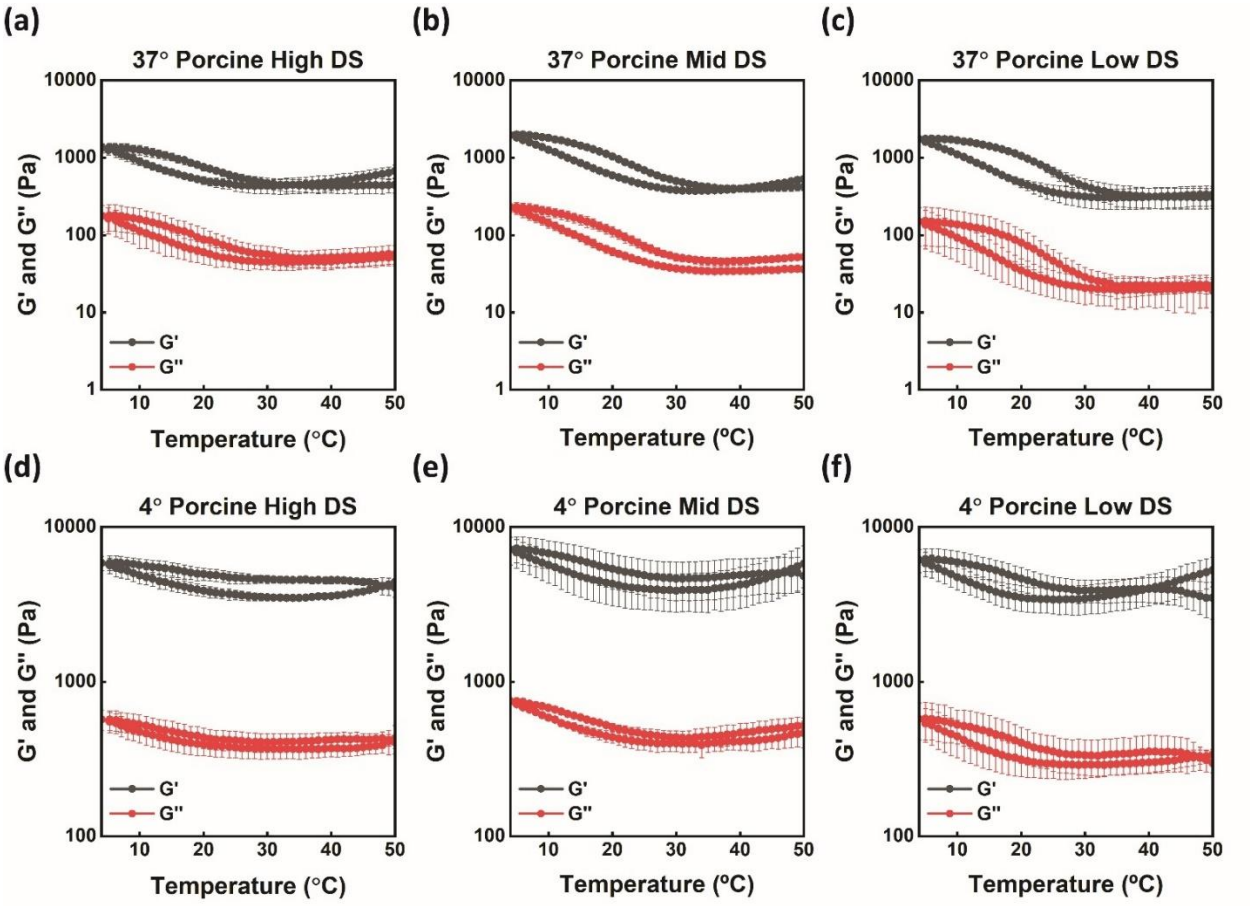


**Figure S8.** Storage modulus (G') and loss modulus (G'') were measured for temperature sweeps from 50°C to 4°C to 50°C for porcine GelMA polymerized at (a) 37°C with high degree of substitution, (b) 37°C with mid degree of substitution, (c) 37°C with low degree of substitution, (d) 4°C with high degree of substitution, (e) 4°C with mid degree of substitution, and (f) 4°C with low degree of substitution.

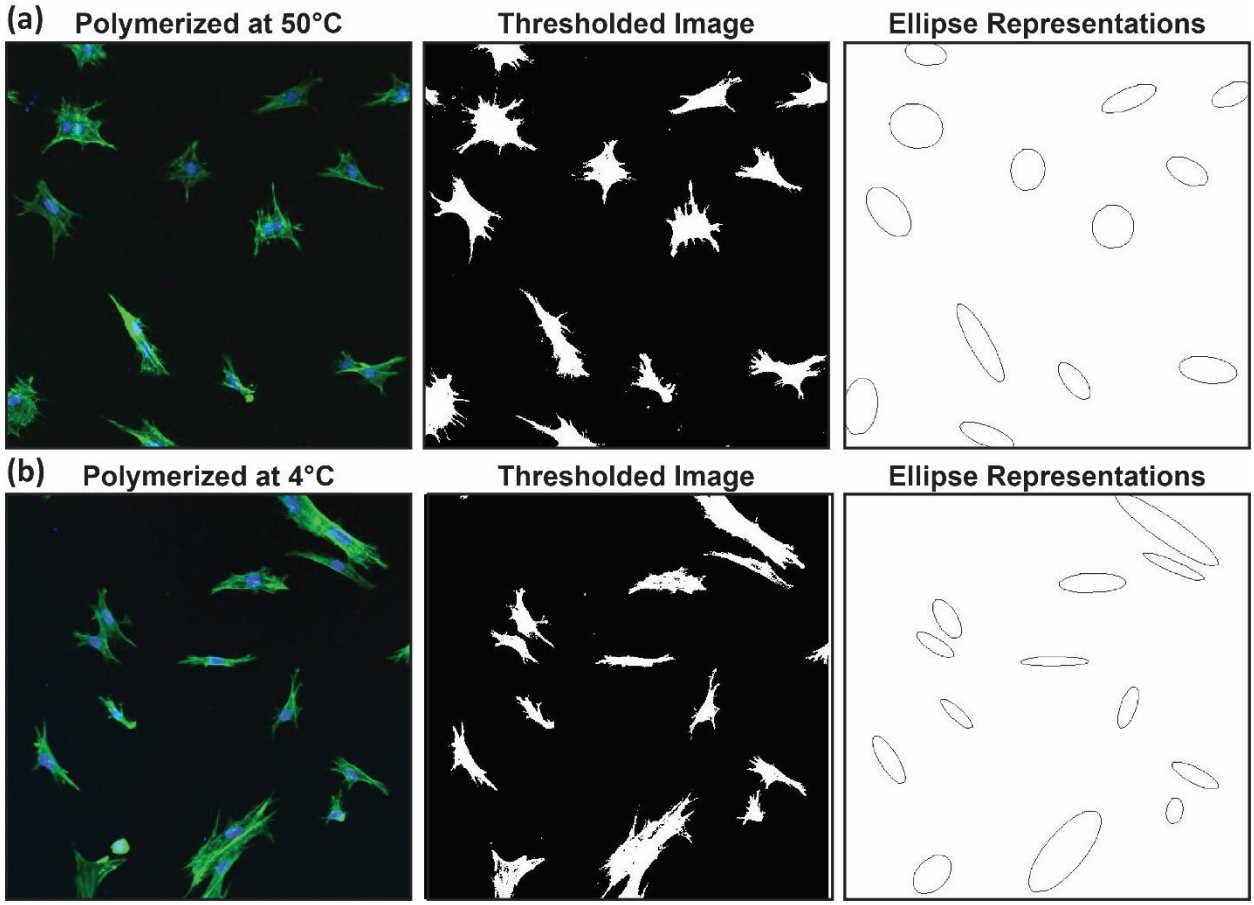


**Figure S9.** Aspect ratio was measured for HDFns cultured on GelMA polymerized at (a) 50°C and (b) 4°C by using thresholding phalloidin-stained cells using ImageJ to isolate cell edges. After thresholding, ellipses were fit to edges and aspect ratio was measured using ImageJ particle analyzer.

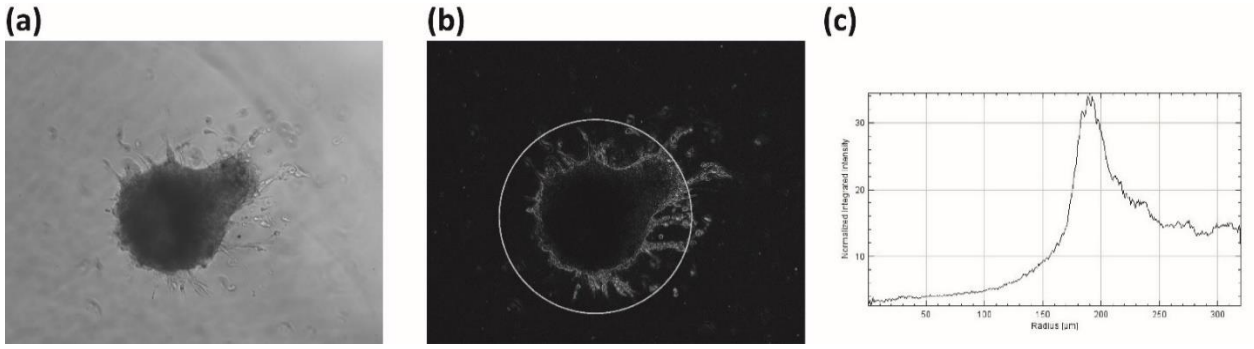


**Figure S10.** Spheroid radius was determined using (a) brightfield images. (b) Edges were determined using ImageJ and the (c) Radial normalized integral intensity was measured. Day 4 spheroid sizes were measured manually using fluorescent confocal images.

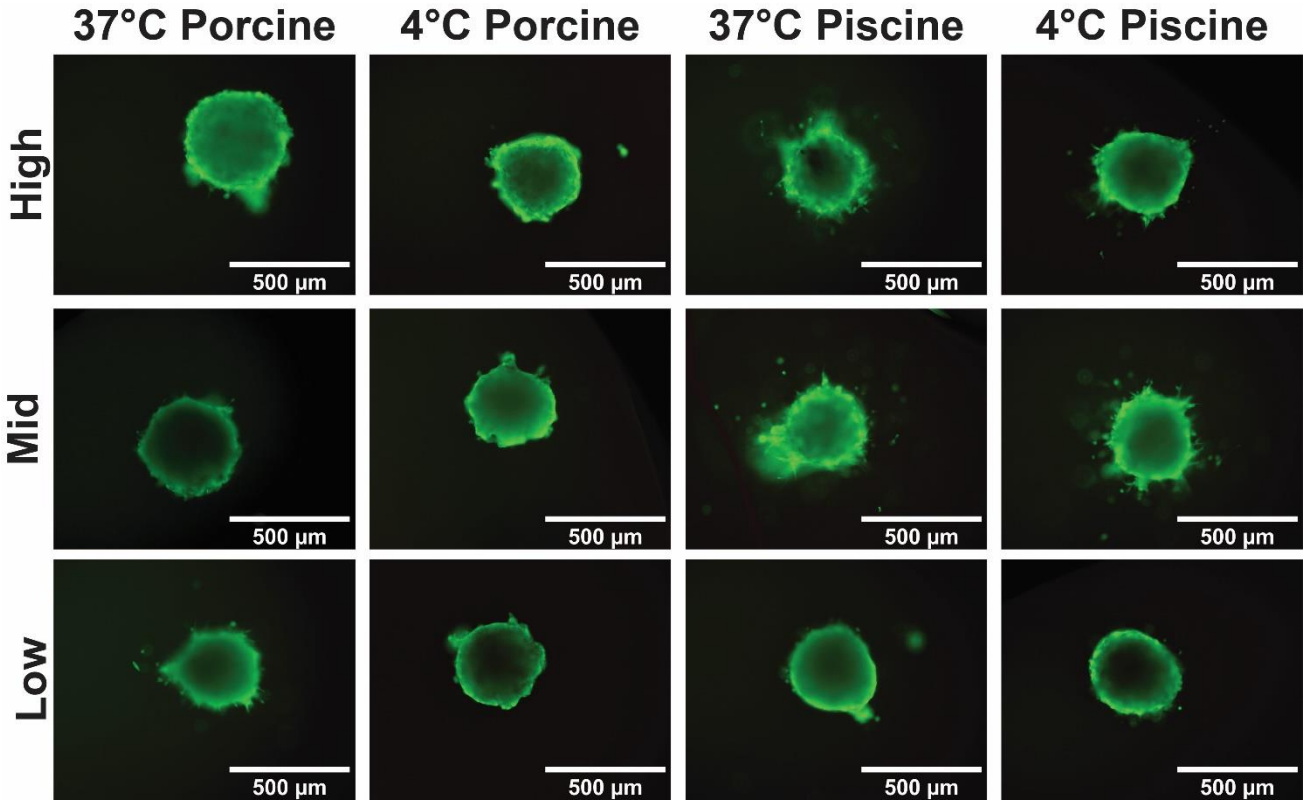


**Figure S11.** MDAMB231 human mammary spheroids were cultured inside GelMA scaffolds of different animal sources, degrees of substitution, and polymerization conditions. Viability was demonstrated using live/dead staining.

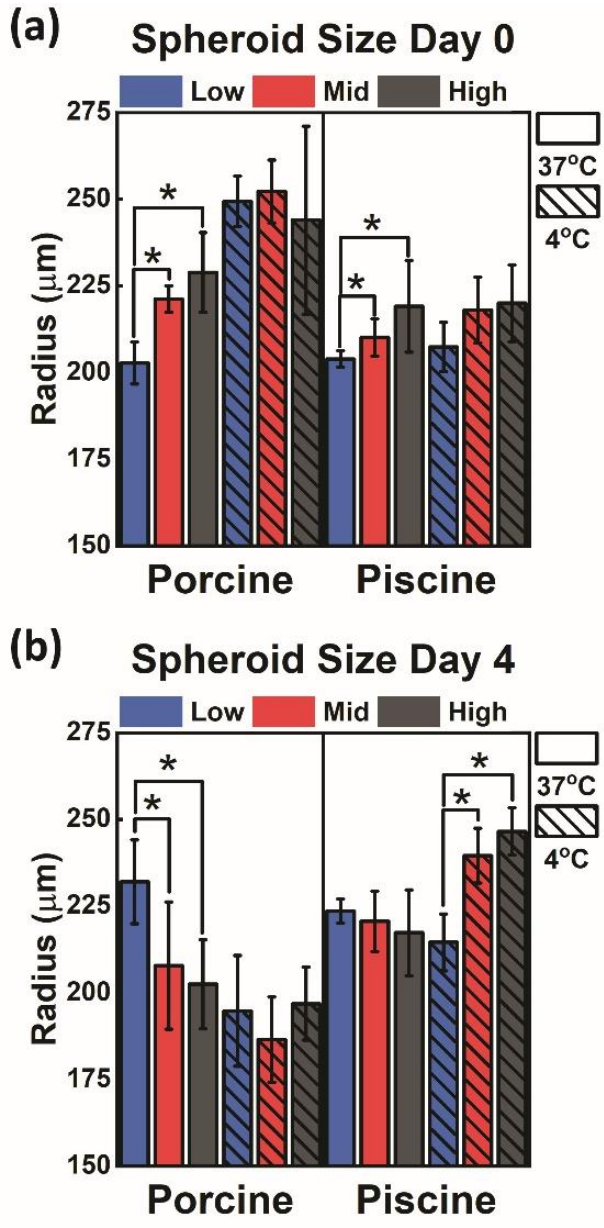


**Figure S12.** Spheroid sizes varied depending on GelMA scaffold degree of substitution when chemically crosslinked alone, quantified as peak radial intensity. (a) Spheroids demonstrated size dependence on GelMA material properties, with stiffer scaffolds generally resulting in larger spheroids. Spheroids were largest in porcine GelMA polymerized at 4°C, regardless of degree of substitution. (b) After four days of growth, Spheroids embedded in porcine GelMA scaffolds with coordinated gelation and crosslinking decreased dramatically. Spheroids embedded in porcine GelMA with chemical crosslinking alone increased in size for the lowest DS, and decreased for mid and high DS. Spheroids embedded in cold-water fish GelMA showed similar traits regardless of crosslinking conditions, and generally increased in size over the four-day period.

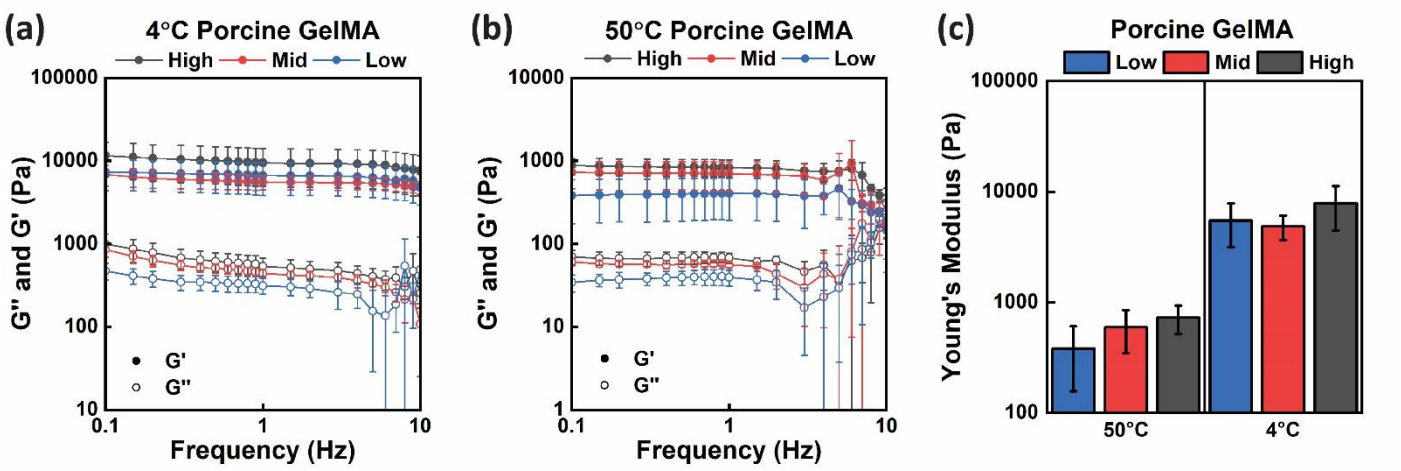


**Figure S13.** Storage modulus (G') and loss modulus (G'') of 6 wt% GelMA with 0.5% photoinitiator from 0.1 Hz to 10 Hz tested at 37°C for (a) porcine GelMA polymerized at 4°C and (b) porcine GelMA polymerized at 50°C for low, medium, and high DS. (c) Young's modulus calculated from the slope of the stress-strain curve for porcine GelMA polymerized at different temperatures and tested at 37°C.